Sustainability, Agri, Food and Environmental Research, (ISSN: 0719-3726), 11(X), 2023:
http://dx.doi.org/10.7770/safer.v11i1.2900

A sustainable approach for synthesis of zinc oxide nanoparticle by *Aloe barbadensis* and its application in photocatalytic decolouration of commercial dyes.

Un enfoque sostenible para la síntesis de nanopartículas de óxido de zinc por *Aloe barbadensis* y su aplicación en la decoloración fotocatalítica de colorantes comerciales.

Riya Shah[*], Nirmal Kumar J.I[1], Rita N Kumar[2], and Nirali Goswami[1]

1- (P.G. Department of Environmental Science and Technology (EST), Institute of Science and Technology for Advanced Studies and Research (ISTAR) –A constituent college of CVM University, India)
2- (Department of Biological and Environmental Science, NV Patel College- A constituent college of CVM University, India)
Corresponding author: shahriya1015@gmail.com

ABSTRACT

The biosynthesis of Zinc oxide nanoparticles (ZnONPs) is gaining popularity as its non- toxic, eco-friendly and biocompatibility makes it environmentally safe and can withstand a wide range of environmental conditions such as pH, temperature The widely known medicinal herb *Aloe barbadensis Miller* was used for synthesis of ZnONPs. XRD (X-Ray Diffraction Analysis), EDAX (Energy dispersive X-ray analysis), and TEM (Transmission Electron Microscopy) were also used to characterise the syntheisis ZnONPs. The XRD and TEM analysis revealed that the synthesised ZnONPs were crystalline in nature, with an average size of 30-50 nm and spherical morphology. The photocatalytic decolorization of Sudan IV, Crystal Violet (CV), and Acridine Orange (AO) dyes under ultraviolet irradiation by biogenically synthesised ZnONPs was studied**.** For all three dyes (10-50 ppm) 100% photocatalytic decolorization was observed in 4-hour incubation time. This biological approach of synthesize of ZnONPs has several advantages over other traditional chemical methods as this is cost effective, highly efficient method.
Keywords: Nanotechnology, Biogenic Synthesis, Zinc Oxide, Photocatalysis, Dye Decolouration

RESUMEN

La biosíntesis de nanopartículas de óxido de zinc (ZnONPs) está ganando popularidad ya que su biocompatibilidad y no tóxica, ecológica y ecológica la hace ambientalmente segura y puede soportar una amplia gama de condiciones ambientales como el pH, la temperatura. La ampliamente conocida hierba medicinal Aloe barbadensis Miller se utilizó para la síntesis de ZnONPs. XRD (X-Ray Diffraction Analysis), EDAX (Energy dispersive X-ray analysis) y TEM (Transmission Electron Microscopy) también se utilizaron para caracterizar los ZnONPs de síntesis. El análisis XRD y TEM reveló que los ZnONPs sintetizados eran de naturaleza cristalina, con un tamaño promedio de 30-50 nm y morfología esférica. Se estudió la decoloración fotocatalítica de los colorantes Sudán IV, Violeta cristalina (CV) y Naranja Acridina (AO) bajo irradiación ultravioleta mediante ZnONPs sintetizados biogénicamente. Para los tres colorantes (10-50 ppm) se observó una decoloración fotocatalítica del 100% en un tiempo de incubación de 4 horas. Este enfoque biológico de síntesis de ZnONPs tiene varias ventajas sobre otros métodos químicos tradicionales, ya que este es un método rentable y altamente eficiente.

Palabras Clave**:** Nanotecnología, Síntesis Biogénica, Óxido de Zinc, Fotocatálisis, Decoloración de Colorante

INTRODUCTION

In recent years, nanotechnology has emerged as a pioneer in a number of industries. Nanomaterials are intensively investigated in numerous sectors such as food, textile, cosmetics, electronics, medical sciences, energy, construction, and environmental remediation due to their unique physicochemical features compared to bulk materials (Varadavenkatesan *et al.*, 2020). Zinc oxide nanoparticles (ZONPs) are a type of precious metal oxide nanoparticle that has gained a lot of interest recently because of its unique properties such as broad bandgap, catalytic effectiveness, and nontoxic nature. Adsorbents, photocatalysts, antimicrobial agents, drug delivery agents, self-cleaning agents, and semiconductors are all common uses for ZONPs (Mirzaei and Darroudi, 2017).

ZnO is a broad band gap semiconductor with an energy band gap of 3.37 eV. ZnO NPs, which have a higher surface area than other metallic nanoparticles (NPs), which is used in a variety of catalytic applications, because of its antibacterial and anti-oxidant characteristics (Walters *et al.,* 2017). ZnO are being manufactured on a commercial scale for agricultural, skin protection, and aesthetic applications (Kaur *et al*., 2021). Physical and chemical approaches for syntheis of ZnONPs, has shown hurdles in terms of environmental toxicity and challenging operating circumstances. For the past few decades, ZnONPs *via* a plant biomimetic pathway have been used as a green and unique method. The photosynthetic approach for ZnO NPs is environmentally friendly and cost-effective, proving its ability to replace chemical and physical routes (Uzair *et al*., 2020). Few examples of green resources used for the preparation of ZONPs include *Linum usitatissimum* (Alkasir *et al*., 2020), *Moringa oleifera* (Letsholathebe *et al*., 2021), *Salvadora persica* (Hamidian *et al*., 2022), *Sambucus spp*. (Vinayagam *et al*., 2021) *Abelmoschus esculentus* (Keerthana *et al*., 2021) and *Peltophorum pterocarpum* (Vinayagam *et al.*, 2021).

Industrial dye effluents in wastewater are a major environmental concern (Verma *et al*., 2021). Crystal Violet, Acridine Orange and Sudan IV are examples of commercial dyes with wide-ranging applications in the textile, paper, and pharmaceutical industries. It is vital that the dye be removed completely before the waters enter the aquatic bodies, as the dye causes serious ecological and health risks (Kishor *et al.,* 2021). The breakdown of dyes in industrial wastewaters has received a lot of interest due to their huge production volume, slow biodegradation, low decolorization, and high toxicity (Kishor *et al.,* 2021)

Therefore, the current study is focused on the (1) fabrication of ZONPs by using *Aloe barbadensis Miller* (2) characterization (3) Photocatalytic ability to decolorize a model pollutant—Acridine Orange, Crystal Violet and Sudan IV dyes in the presence of Ultraviolet irradiation.The effects of different operational parameters as pH and catalytic dosage on the decolouration of dyes were studied.

MATERIAL AND METHODS

All of the chemicals and reagents used in the synthesis of ZnO nanoparticles are of analytical grade and were supplied by Merck India Ltd., Banglore

Aloe barbadensis Miller extract preparation

The leaves of what? were collected from the campus of Anand Agriculture University (Anand, India). The leaves of the *Aloe vera* plant were plucked from the plant and thoroughly cleansed with double distilled water before being sliced with sharp knife into little pieces. 25g of leaves were boiled in 100ml of distilled water with for 2 hours at 90°C (Bachheti *et al*., 2021).

Fabrication of ZnO spherical nanoparticle

The *Aelo vera* extract was filtered using Whatman filter paper No. 41. The filtrate was preserved and used to synthesis nanoparticles. Using magnetic stirrer (Sesw 2L), the extract was heated to 60-80°C. When the temperature reached 70°C, 5 g of Zinc Nitrate was added to the leaf extract and was well stirred for 1hr. This mixture was then dried for around 2 hrs in a Hot Air Oven at 105°C. Then it was calcined for 30 minutes in a Muffle furnace

at 400°C (Bachheti *et al*., 2021). The particles were then crushed and grinded in a mortar and pestle to obtain fine powder (Figure 1).

Photocatalytic activity for Decolouration of Commercial Dyes

Erlenmeyer flask containing dye were kept in the dark for 30 minutes to determine consistent dye degradation. Experiments were carried out in a 100 mL flask that was wrapped with aluminium foil to eliminate the contamination of foreign particles (Soni *et al*., 2016). The effects of pH, initial concentration and catalyst dosage were investigated for different isotherms with concentrations ranging from 10, 20, 30, 40, and 50 ppm The pH ranges selected for optimization of acidity and alkanlinity function was 3, 6, 9, and 12, with 5mg of ZnONPs nanoparticles, The dye was treated with ZnO nanoparticles with 5, 10, 15, 20, 25, and 30mg dosages, the dose that resulted in maximum decolouration was selected as the optimum dose for further experiment. 20 ml Acridine Orange, Crystal Violet and Sudan IV dyes were extracted from flasks and placed in test tubes, each with optimized catalyst dosage. Tubes containing catalyst were placed on the UV-radiation surface in slanted direction. Low-pressure mercury UV tubes (Spectronics), each with 15 watts, producing near-ultraviolet radiation at a wavelength of 365 nm. Photocatalysis is used to catalyse oxidation. When UV photons reached ZnO, the photocatalyst reaction began. The tubes were then gently swirled every now and then to agitate them. At 30 miniutes interval, temperature and pH were measured. The samples were centrifuged for 4–5 minutes at 950–1,000 rpm, and their absorbance was measured at 520 nm (Sudan IV), 690 nm (Crystal Violet), and 494 nm (Acridine Orange) with a UV-Visible spectrophotometer (Systronic 118) (Alasel *et al.,* 2017; Papadimitriou *et al.,* 2019; Kostjukova *et al.,* 2021) The photodegradation efficiency was evaluated using the equation:

$$\text{Photodegradation efficiency} = \frac{\text{Initial OD} - \text{Final OD}}{\text{initial OD}} \times 100 \quad (1)$$

For characterization of biogenic ZnONPs were subjected to different sophisticated instrumental methods such as X-ray diffraction (XRD), transmission electron microscopy (TEM), EDAX (Energy dispersive X-ray microanalysis) (Kumar *et al.*, 2022). Approximately 0.5 g of dry ZnONPs were randomly orientated in a Plexiglas sample container, and XRD patterns were recorded between 20 and 80 degree angles. The XRD patterns were compared using anase diffractograms. A transmission electron microscope (TEM) with a 100 kV accelerating voltage, model Philips Tecnai 20, Holland, was used to examine the form and size of the particles. The samples were placed on carbon-coated copper grids for TEM examination. The particles were dispersed in 2-propanol for sample preparation . EDAX was used for element analysis, with a voltage of 30 kV and magnification of up to 2,50,000x. All physicochemical analysis were performed in SICART (Sophisticated Instrumentation Centre for Applied Research and Testing, Vallabh Vidyanagar, Anand)

RESULT AND DISCUSSION

Characterization of Biogenic Zinc Oxide Nanoparticles

Energy Dispersive X-ray Analysis (EDAX)

The EDAX spectra (Fig. 3C) showed the presence of Zinc (64.99%) and Oxygen (17.47%) with Sodium (15.63%), Magnesium (0.96%), Potassium (0.43%), Calcium (0.52%) to be specific, strong peaks of Zn observed at 8.6 keV and 1 keV. Similarly, O exhibited a strong signal at 0.5 keV. Therefore, the existence of these signals corroborated the synthesis of ZnO nanoparticles. The Na, Ca, and Mg signals might be because of the interference of phytochemicals during the synthesis of biogenic ZnO nanoparticles (Pai *et al*., 2019). The higher weight percentage of Zn and O confirms the presence of ZnO nanoparticles (Figure 2).

Xray Diffraction analysis (XRD)

Strong intense and narrow width of diffraction peaks of ZnO nanoparticles indicates that they are highly crystalline in nature at peak angle of 31.782, 34.447, 36.271, 47.558, 56.596, 62.864 in correspondance with the Miller indices (1 0 0), (0 0 2), (1 0), (1 0 2), (1 1 0), (1 0 3), (1 1 2), (2 0 1), and (2 0 2), which were accurately indexed

to the pure hexagonal wurtzite phase of zinc oxide nanoparticles (JCPDS Card No.: 36–1451). (Ekennia *et al*., 2020).The nanoparticles' high crystalline nature was revealed by the sharp and distinct diffraction patterns. There was no further contamination observed. The Debye–Scherrer equation predicted a mean crystallite size of 36.271 nm . Accordingly, Scherrer's formula, which is given by equation:

$$d = k\lambda / (\beta\cos\theta) \quad (2)$$

where d is the crystal size; k is the X-ray radiation wavelength (k = 0.15406 nm) for Cukα; k is commonly chosen as 0.89; and b is the line width at half-maximum height, can be used to compute the particle size of the produced nanomaterials. Because of the reduced crystallite size, the diffraction peaks are wider (Figure 3).

Transmission Electron Microscopy analysis (TEM)

The NPs of ZnO were agglomerated irregular spherical morphology (Figure 4A) with an average size of about 30-50 nm for biogenic synthezised ZnO, similar results were observed by Cruz (2020). The particle size of ZnO nanoparticles determined by TEM analysis. It is found to be fairly compatible with the particle size calculated by XRD analysis. The Selected Area Electron Diffraction (SAED) pattern of ZnO nanoparticles is shown in Figure 4B. The existence of concentric Scherrer's rings that reveal orientation in all directions indicates the creation of ZnO nanoparticles.

Photocatalytic Decolouration

Alkalinity and Acidity Function

Changes in acidity and alkalinity function were studied in relation to initial dye concentration under normal light conditions. The dye's pH was investigated because it is one of the most crucial factors that can influence the photocatalytic breakdown process. The initial pH of the dyes was adjusted from 3 to 9. Experiments on pH 12 were also conducted, however the cause of decolouration due to the addition of excessive NaOH was observed and therefore pH 12 was not considered. The further experiment on pH was carried out with 10, 20, 30, 40, and 50 ppm of Sudan IV, Crystal Violet, and Acridine orange dye solutions , as well as a 5 mg catalyst dosage (Figure 5).

The influence of pH on Sudan IV adsorption was investigated, and it was found out that the optimum pH for dye adsorption is 3 (Sajjala *et al*., 2020), which is roughly 26 percent. Therefore, one can conclude that Sudan IV dye has a low absorption ability in alkaline medium. The maximum amount of decolouration for Crystal Violet and Acridine Orange dyes was 28 percent and 28 percent, respectively, at pH 9 (Abbas et al., 2020; Hasanpour *et al.,* 2020). Photocatalytic decolouration of Crystal Violet and Acridine may occur in acidic pH because several hydroxyl ions increase at higher pH values, resulting in increased decoloration.

Effect of Initial Dye Concentration

The initial dye concentration was also referred to in the experimental design during the pH optimization by selecting concentrations of 10, 20, 30, 40, and 50 mg/L, where decoloration decreased as concentration increased (Paul *et al*., 2020) (Figure 5) because some UV light photons were absorbed by a large number of dye molecules as the dye concentration increased. The quantity of photons absorbed by the surface of the catalyst was reduced. The size of the generating electrons and photon holes shrank as the quantity of excited biogenic ZnO electrons generated by effective photons decreased. Contaminants and other organic molecules were likely accumulated on the ZnO surface at the same time, making it harder for electrons and holes to enter the solution.As a result, less and fewer electrons reached the dye solution, where they reacted with adsorbed hydroxide ions to form hydroxyl radicals, the most important oxidizing species in organic compound photooxidation.

Effect Of Catalyst Loading

Following pH optimization, catalyst loading is another critical parameter that has a significant impact on dye solution decoloration kinetics. A series of tests were carried out utilizing different amounts of ZnO catalyst ranging from 5, 10, 15, 20, 25, and 30 mg at adjusted pH and beginning dye concentration under normal light conditions in order to determine the optimal quantity of catalyst concentration. Increased dye decoloration was

found when the catalyst concentration was increased from 5mg to 10mg. Further investigation revealed a decrease in dye decoloration (Figure 6). This increases the possibility of a surplus catalyst scattering photons in a photoreaction system (Zeng *et al*., 2019). This could be due to active molecules interacting with ZnO ground state molecules, which causes them to become deactivated.

Photocatalytic Decolouration under Ultraviolet Radiation

The decolouration of 3 organic dyes Sudan IV, Crystal Violet and Acridine Orange dye solution under UV light irradiation at room temperature was used to test the photo catalytic characteristics of the as-prepared samples. However, optimized pH 9 for Acridine Orange and Crystal Violet and pH 3 for Sudan IV with catalytic dosages 10 mg, were used to irradiate five dye concentrations: 10 ppm, 20 ppm, 30 ppm, 40 ppm, and 50 ppm. To uncover possible dye losses in the system, control experiments were carried out without the inclusion of the catalyst. In the course of photo catalytic decolouration of three commercial dyes, pure catalyst ZnO was applied to different dye concentrations. No noticeable loss was observed in the control experiment, indicating that the dyes were stable in our study. During our testing, we witnessed complete elimination of all three dyes. Different dye concentrations were found to completely decolorize the dyes Figure 7 shows that for Sudan IV dye 40 and 50ppm dye concentrations, % decolouration occurred in 2 hours and % removal occurred in 4 hours for all dye concentrations. For 10 and 20ppm dye concentrations, roughly 80-85 % removal was recorded in 3 hours, but for 10, 20, and 30 ppm dye concentrations, % removal was detected after 4 hours of irradiation, with around 90% removal for 40 and 50ppm concentrations (Figure 8).

Out of all three dyes, Acridine Orange decolorization was the fastest, with 95%-90 % removal for 10 and 20 ppm of dye in 3 hours of irradiation, and almost 75-80 % removal for 30, 40, and 50 ppm of dye concentration in 3 hours (Figure 9). Complete decolouration for Crystal Violet 10, 20, 30 ppm, and Sudan IV 10 and 20ppm was observed with around 90% removal for 30, 40, and 50ppm concentrations with biogenic ZnO nanocatalyst in 4hrs of irradiation time for acridine Orange, whereas complete decolouration for Crystal Violet 10, 20, 30ppm, and Sudan IV 10 and 20ppm was observed with around 90-% removal for 30, 40, and 50ppm concentrations with biogenic ZnO.

Adsorption Isotherm

For analysing experimental equilibrium parameters, Langmuir and Freundlich models are the most widely employed isotherm equations. The Langmuir isotherm model is based on the assumption that the adsorbent's surface has a finite number of active sites that are uniformly distributed. Because these active sites have the same proclivity for adsorption as a monomolecular layer, there is no interaction between the adsorbed molecules. Adsorption isotherms depict the equilibrium relationship between the bulk activity of adsorbate in solution and the moles adsorbed onto the surface at constant temperature. The adsorption isotherm (Freundlich and Langmuir) connects the equilibrium adsorbate concentration in the bulk to adsorbate absorption on the adsorbent surface and optimally describes the adsorption characteristics for a wide range of adsorbate concentrations (Ewis *et al*., 2020).

The separation factor "RL," a significant characteristic of the Langmuir adsorption isotherm, was used to describe the affinity of nanoparticles for Dye (Fegade et al., 2019). Sudan IV, Crystal Violet, and Acridine Orange dyes have RL values of 0.0635, 0.2679, and 0.1126, respectively (Table I). The values of RL reclining in the range of 0 to 1 showed that the adsorption was favourable. The significance of the n value is that it denotes the adsorption nature in the Freundlich adsorption isotherm (Table II) The importance of n is as follows: n = 1, adsorption is linear; n 1, adsorption is chemical; n >1, adsorption is physical. In the current investigation, the value of n in the Freundlich isotherm was determined to be in the range of 0 to 1. The value of n in the Freundlich isotherm in this investigation was found to be in the range of 0 to 2, indicating that the adsorption was physisorption for Sudan IV and chemosorption for Acridine Orange Dye. Both Langmuir and Freundlich values indicated that dye adsorption onto the adsorbent was fast and had a large adsorption capacity. The R2 value of the graph, on the other hand, indicates the experiment's accuracy.

Photocatalytic mechanism

The incident ultraviolet radiations have more energy than the band gap energy of ZnONPs. Therefore, as depicted in Figure10 the photocatalytic mechanismdye, it involves the creation of electrons (e–) in the conduction band (CB) and holes (h+) in the valance band (VB) when ultraviolet irradiates on the surface of ZnONPs. These generated e– converts dissolved O2 to form superoxide free radicals (O2–) and h+ produce ·OH free radicals. These intermediates are highly active which act as oxidizing and reducing agents and thus are responsible for the photodecolouration of dyes as explained by Vinayagam (2021).

As conclusion, the capacity of Biogenically synthesised ZnO nanoparticles for removal of commercial dyes was examined in this paper where optimization of pH, Dosage plays significant role where Sudan IV dye decolouration was more efficient in acidic pH 3 and that for Crystal Violet and Acridine Orange was in alkaline medium pH 9. The synthesis process was found to be important in the development of ZnO with particle sizes of 30-50 nm, respectively. It was found that biogenic ZnO has a spherical irregular morphology. Whereas, the higher weight percentage of Zn and O and traces of Na, Ca, Mg in EDAX analysis confirms the presence of biogenic ZnO.Under UV light, this biogenic catalyst derived from aloe extract was able to totally decolorize the dye in 4 hours. When compared to Sudan IV, the decolorization in Acridine Orange and Crystal Violet was twice as quick. The data are accurately represented by the Freundlich and Langmuir isotherms, revealing that adsorption by the adsorbent is favourable. Biogenic ZnO has substantial promise as an adsorbent for the removal of organic dyes, according to the findings, and can be employed commercially as an adsorbent due to its environmental friendliness.

REFERENCES

Varadavenkatesan, T., Selvaraj, R., and Vinayagam, R. (2020). Green synthesis of silver nanoparticles using Thunbergia grandiflora flower extract and its catalytic action in reduction of Congo red dye. *Materials Today: Proceedings*, 23: 39 - 42.

Mirzaei, H., and Darroudi, M. (2017). Zinc oxide nanoparticles: Biological synthesis and biomedical applications. *Ceramics International*, 43 (1): 907 - 914.

Walters, C. R., Cheng, P. H., Pool, E. J., and Somerset, V. S. (2017). Combined silver nanoparticles and temperature effects in the Cape River crab *Potamanaut esperlatus*, *interactions between chemical and climatic stressors*, 6(2): 1 - 9

Kaur, R., Bhardwaj, S. K., Chandna, S., Kim, K. H., and Bhaumik, J. (2021). Lignin-based metal oxide nanocomposites for UV protection applications: A review. *Journal of Cleaner Production*, 317:128300.

Uzair, B., Liaqat, A., Iqbal, H., Menaa, B., Razzaq, A., Thiripuranathar, G., and Menaa, F. (2020). Green and cost-effective synthesis of metallic nanoparticles by algae: Safe methods for translational medicine. *Bioengineering*, 7(4): 129.

Abbasi, B. H., Anjum, S., and Hano, C. (2017). Differential effects of in vitro cultures of *Linum usitatissimum.*(Flax) on biosynthesis, stability, antibacterial and antileishmanial activities of zinc oxide nanoparticles: a mechanistic approach. *RSC advances*, *7*(26): 15931 - 15943.

Letsholathebe, D., Thema, F. T., Mphale, K., Maabong, K., and Magdalane, C. M. (2021). Green synthesis of ZnO doped Moringa oleifera leaf extract using Titon yellow dye for photocatalytic applications. *Materials Today: Proceedings*, 36: 475 - 479.

Hamidian, K., Sarani, M., Sheikhi, E., and Khatami, M. (2022). Cytotoxicity evaluation of green synthesized ZnO and Ag-doped ZnO nanoparticles on brain glioblastoma cells. *Journal of Molecular Structure*, 1251: 131962.

Vinayagam, R., Pai, S., Murugesan, G., Varadavenkatesan, T., and Selvaraj, R. (2021). Synthesis of photocatalytic zinc oxide nanoflowers using *Peltophorum pterocarpum* pod extract and their characterization. *Applied Nanoscience*, 1-11.

Keerthana, P., Vijayakumar, S., Vidhya, E., Punitha, V. N., Nilavukkarasi, M., andPraseetha, P. K. (2021). Biogenesis of ZnO nanoparticles for revolutionizing agriculture: A step towards anti-infection and growth promotion in plants. *Industrial Crops and Products*, *170*: 113762.

Verma, R. K., Sankhla, M. S., Rathod, N. V., Sonone, S. S., Parihar, K., and Singh, G. K. (2021). Eradication of fatal textile industrial dyes by wastewater treatment. *Biointerface Research. Applied. Chemistry*, 12: 567 - 587.

Kishor, R., Purchase, D., Saratale, G. D., Saratale, R. G., Ferreira, L. F. R., Bilal, M., and Bharagava, R. N. (2021). Ecotoxicological and health concerns of persistent coloring pollutants of textile industry wastewater and treatment approaches for environmental safety. *Journal of Environmental Chemical Engineering*, 9(2):105012.

Bachheti, A., Bachheti, R. K., Abate, L., and Husen, A. (2021). Current status of Aloe-based nanoparticle fabrication, characterization and their application in some cutting-edge areas. *South African Journal of Botany,* 00(2021):1 - 12 Incomplete reference

Soni, H., Kumar, J. N., Patel, K., and Kumar, R. N. (2016). Photocatalytic decoloration of three commercial dyes in aqueous phase and industrial effluents using TiO_2 nanoparticles. Desalination and Water Treatment, 57(14): 6355 - 6364.

Alasel, M., and Keusgen, M. (2017). A new platform for serological analysis based on porous 3-dimensional polyethylene sinter bodies. *Journal of Pharmaceutical and Biomedical Analysis*, 145: 110 - 118.

Papadimitriou, M., Hatzidaki, E., and Papasotiriou, I. (2019). Linearity comparison of three colorimetric cytotoxicity assays. *Journal of Cancer Therapy*, 10(07): 580.

Kostjukova, L. O., Leontieva, S. V., and Kostjukov, V. V. (2021). The vibronic absorption spectra and electronic states of acridine orange in aqueous solution. *Spectrochimica Acta Part A: Molecular and Biomolecular Spectroscopy*, 249:119302.

Kumar, S., Sharma, A., Gautam, D., and Hooda, S. (2022). Characterization of Mesoporous Materials. In Advanced Functional Porous Materials. *Springer, Chemistry and Materials Science,* 797: 175 - 204 .

Pai, S., Sridevi, H., Varadavenkatesan, T., Vinayagam, R., and Selvaraj, R. (2019). Photocatalytic zinc oxide nanoparticles synthesis using Peltophorumpterocarpum leaf extract and their characterization. *Optik*, 185: 248 - 255.

Ekennia, A. C., Uduagwu, D. N., Nwaji, N. N., Oje, O. O., Emma-Uba, C. O., Mgbii, S. I., and Nwanji, O. L. (2021). Green synthesis of biogenic zinc oxide nanoflower as dual agent for photodegradation of an organic dye and tyrosinase inhibitor. *Journal of Inorganic and Organometallic Polymers and Materials*, 31(2): 886 - 897.

Cruz, D. M., Mostafavi, E., Vernet-Crua, A., Barabadi, H., Shah, V., Cholula-Díaz, J. L., ... and Webster, T. J. (2020). Green nanotechnology-based zinc oxide (ZnO) nanomaterials for biomedical applications: A review. *Journal of Physics: Materials*, 3(3): 034005.

Sajjala, S. R., and Sairam, V. (2020). De-Colorization of Sudan IV Dye Solution by Solar Photo Fenton and TiO2 Mediated Solar Photo Fenton Processes: A Comparative Study. *International Journal of Advanced Research in Engineering and Technology*, 11(6): 774 – 785.

Abbas, H. A., Nasr, R. A., Abu-Zurayk, R., Al Bawab, A., and Jamil, T. S. (2020). Decolourization of crystal violet using nano-sized novel fluorite structure Ga2Zr2− x W x O7 photocatalyst under visible light irradiation. *Royal Society open science*, 7(3): 191632.

Hasanpour, M., and Hatami, M. (2020). Photocatalytic performance of aerogels for organic dyes removal from wastewaters: Review study. *Journal of Molecular Liquids*, *309*, 113094.

Paul, J. J., Surendran, A., andThatheyus, A. J. (2020). Efficacy of orange peel in the decolourization of the commercial auramine yellow dye used in textile industry. *Indian Journal of Biochemistry and Biophysics (IJBB)*, 57(4): 481 - 485.

Zeng, B., Liu, W., Zeng, W., andJin, C. (2019). Carbon Nanotubes-Wrapped Urchin-Like Bi2S3 Composites with Enhanced Photocatalytic Performance. *Journal of Nanoscience and Nanotechnology*, 19(4): 2276 - 2280.

Ewis, D., Benamor, A., Ba-Abbad, M. M., Nasser, M., El-Naas, M., andQiblawey, H. (2020). Removal of oil content from oil-water emulsions using iron oxide/bentonite nano adsorbents. *Journal of Water Process Engineering*, 38: 101583.

Fegade, U., Jethave, G., Su, K. Y., Huang, W. R., and Wu, R. J. (2018). An multifunction Zn0. 3Mn0. 4O4 nanospheres for carbon dioxide reduction to methane via photocatalysis and reused after five cycles for phosphate adsorption. *Journal of Environmental Chemical Engineering*, 6(2): 1918 - 1925.

Received: 15th Juny 2022; Accepted: 12th September 2022; First distribution: 29th October 2022.

FIGURES

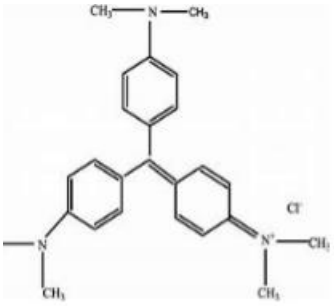

Crystal Violet

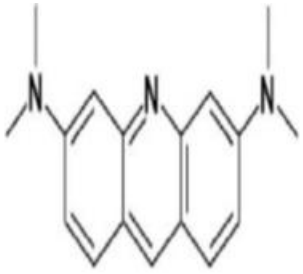

Acridine Orange

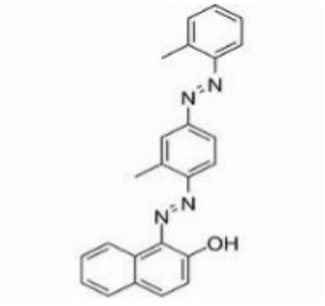

Sudan IV

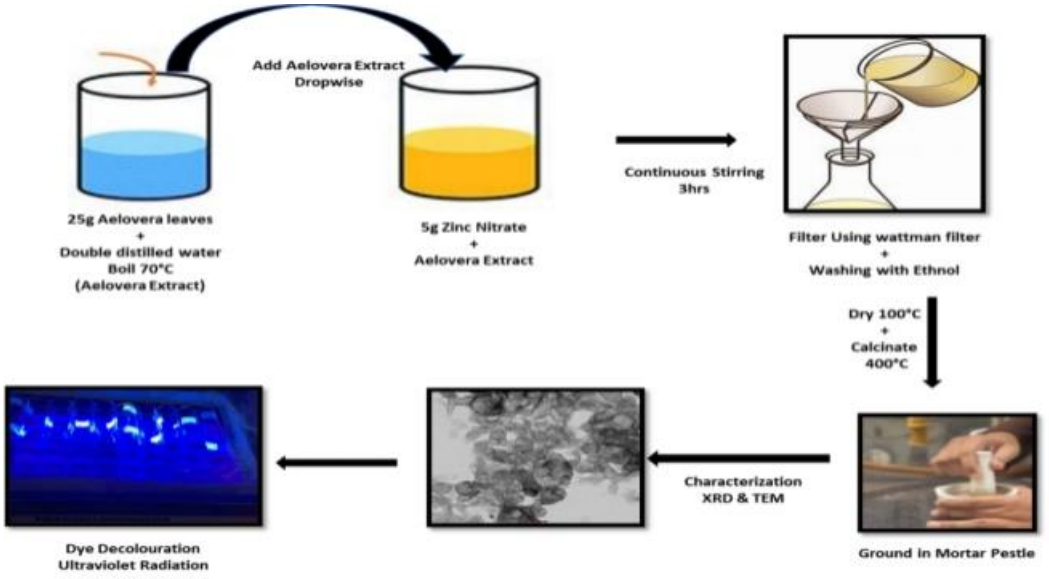

Figure 1 Method for synthesis of Biogenic ZnO

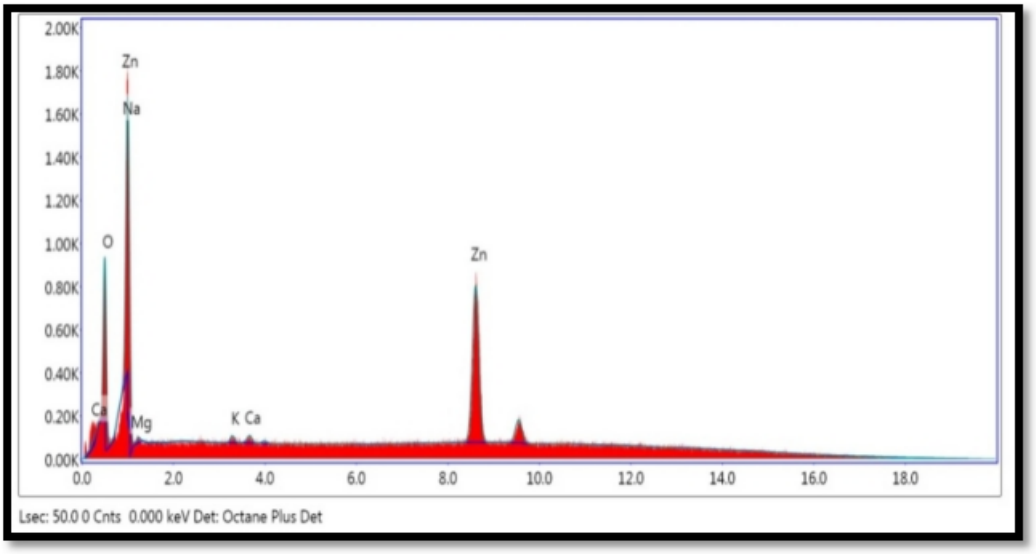

Figure 2 EDAX analysis of Biogenic ZnO

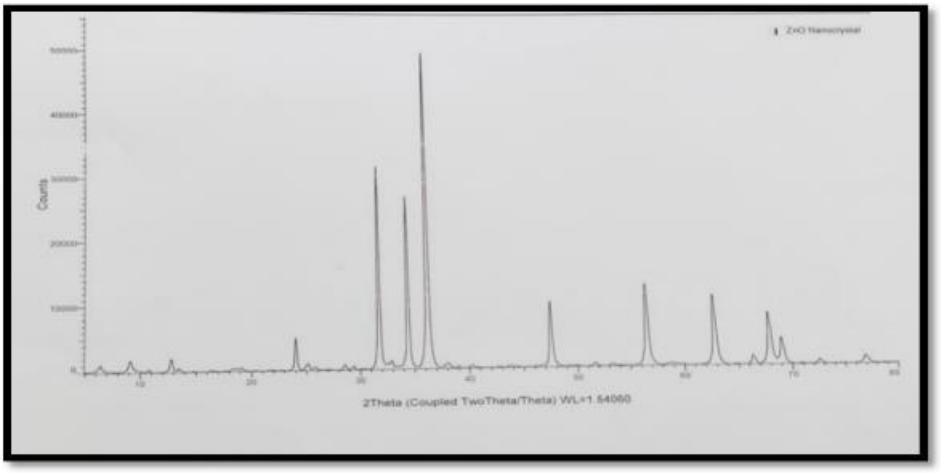

Figure 3 XRD analysis of Biogenic ZnO

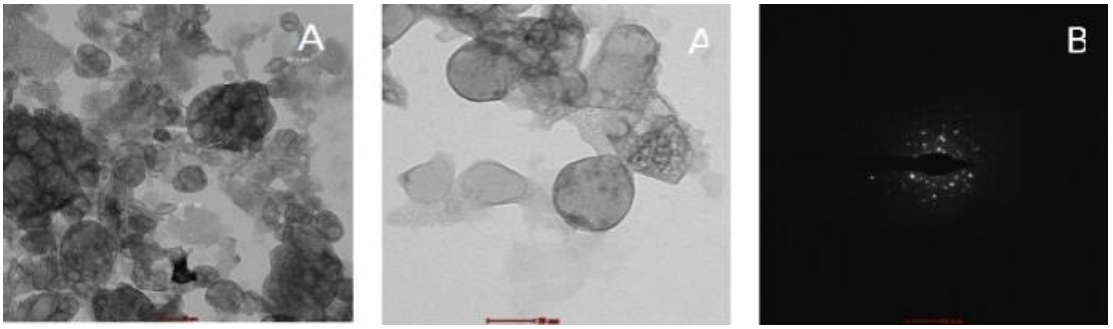

Figure 4 (A) TEM Analysis Of biogenic ZnO (B) SAED pattern Of Biogenic ZnO

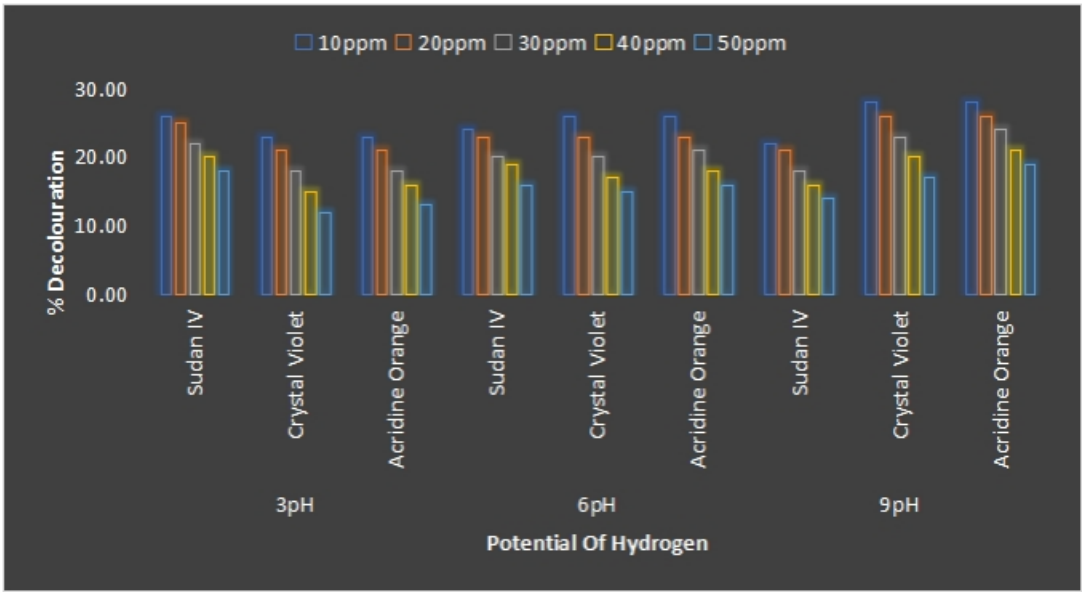

Figure 5 pH Optimization with reference to initial dye concentration

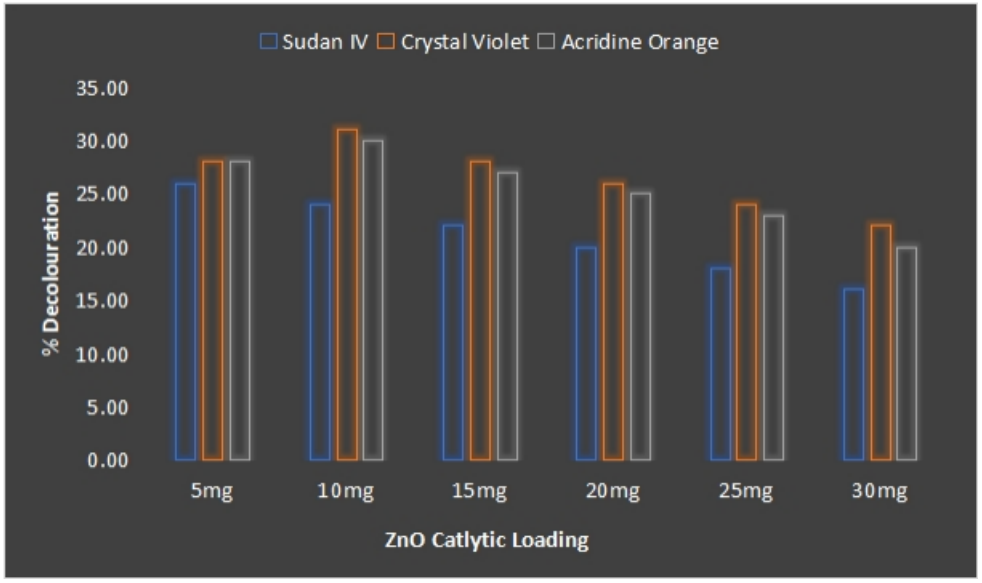

Figure 6 Optimization of Catalytic dosage

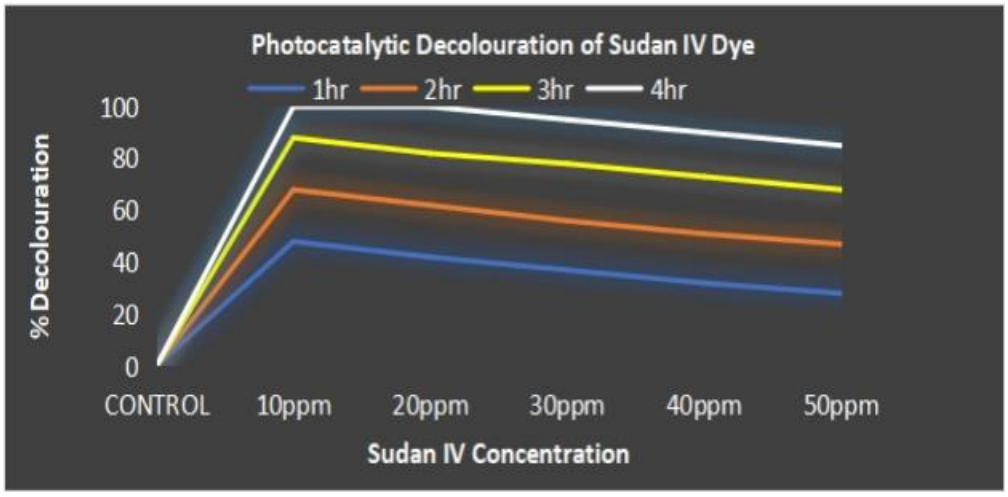

Figure 7 Photocatalytic Decolouration of Sudan IV dye

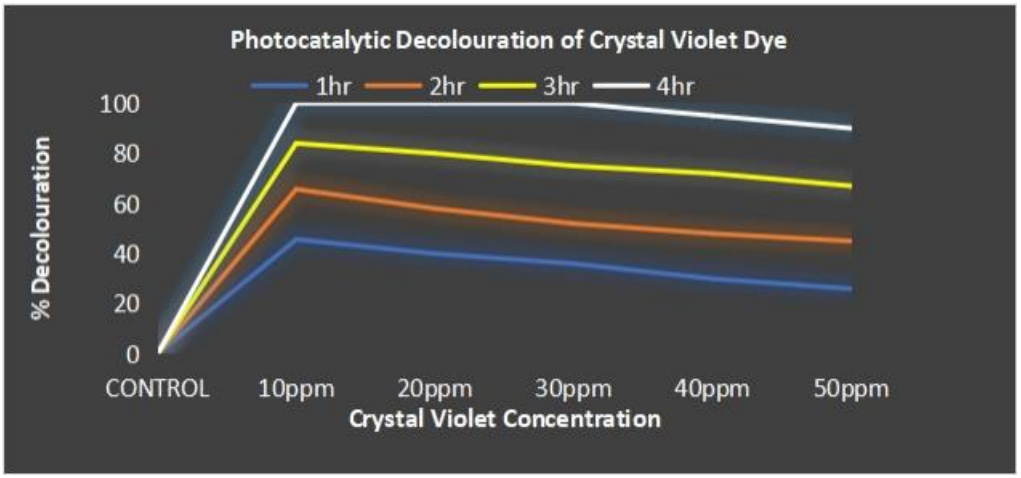

Figure 8 Photocatalytic Decolouration of Crystal Violet dye

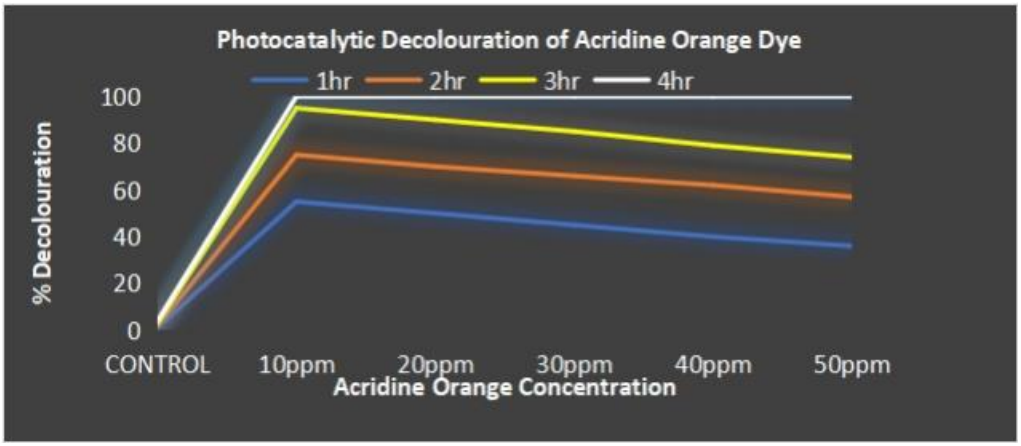

Figure 9 Photocatalytic Decolouration of Acridine Orange dye

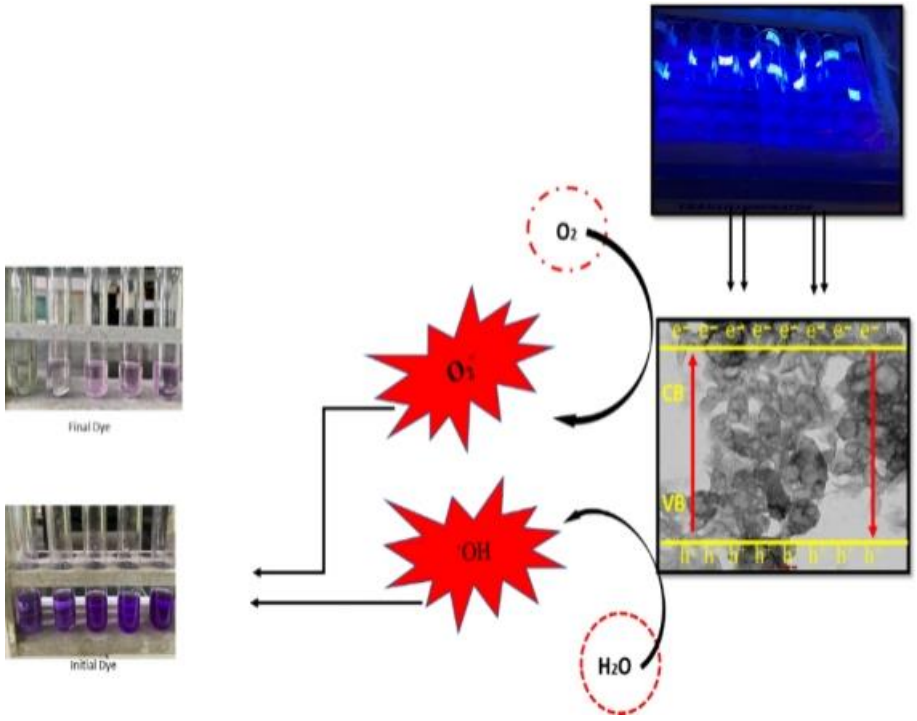

Figure 10 Photocatalytic mechanism

TABLES

Table I Langmuir Adsorption Isotherm

Dye	Intercept	Slope	Qmax	KL	RL	R2
Sudan IV	0.1782	0.2526	5.611672	0.705463	0.124152	0.9803
Crystal Violet	0.2384	0.9390	4.194631	0.253887	0.282576	0.9633

Acridine Orange	0.5876	0.7769	1.701840	0.756340	0.152360	0.9995

Table II Freundlich Adsorption Isotherm

Dye	Intercept	Slope	1/n	Kf	R2
Sudan IV	0.3321	0.509	1.964637	2.148325	0.9747
Crystal Violet	-0.0348	0.5704	1.753156	0.922996	0.9063
Acridine Orange	0.7505	2.6739	0.373986	5.629891	0.9052